

HEARES 01516

## Measuring and modelling the response of auditory midbrain neurons in the grassfrog to temporally structured binaural stimuli

Ivo H.M. van Stokkum and Willem J. Melszen

*Department of Medical Physics and Biophysics, University of Nijmegen, The Netherlands*

(Received 16 April 1990; accepted 22 September 1990)

The combined selectivity for amplitude modulation frequency (AMF) and interaural time difference (ITD) was investigated for single units in the auditory midbrain of the grassfrog. Stimuli were presented by means of a closed sound system. A large number of units was found to be selective for AMF (95%) or ITD (85%) and mostly, these selectivities were intricately coupled. At zero ITD most units showed a band-pass (54%) or bimodal (24%) AMF-rate histogram. At an AMF of 36 Hz, which is equal to the pulse repetition rate of the mating call, 70% of the units possessed an asymmetrical ITD-rate histogram, whereas about 15% showed a symmetrically peaked histogram. With binaural stimulation more units appeared to be selective for AMF (95%) as was the case with monaural stimulation (85%). A large fraction of the units appeared to be most selective for ITD at AMFs of 36 and 72 Hz, whereas units seldomly exhibited ITD selectivity with unmodulated tones. Based upon previous papers (Melszen et al., 1990; Van Stokkum, 1990) a binaural model is proposed to explain these findings. An auditory midbrain neuron is modelled as a third order neuron which receives excitatory input from second order neurons. Furthermore the model neuron receives inputs from the other ear, which may be either excitatory or inhibitory. Spatiotemporal integration of inputs from both ears, followed by action potential generation, produces a combined selectivity for AMF and ITD. In particular the responses of an experimentally observed EI neuron to a set of stimuli are reproduced well by the model.

Anuran; Binaural hearing; Neural modelling; Temporal selectivity; Torus semicircularis

### Introduction

Anurans use stereotyped, species-specific calls for intraspecific communication. In the grassfrog, *Rana temporaria*, these calls possess a periodic

*Abbreviations:* AMF amplitude modulation frequency; BF best frequency; BMF best modulation frequency; CCH simultaneous cross-coincidence histogram; CITD cut-off interaural time difference; CL contralateral; DMN dorsal medullary nucleus; EPSP excitatory post synaptic potential; IID interaural intensity difference; IL ipsilateral; IPSP inhibitory post synaptic potential; ITD interaural time difference; LT latency; MSAM monaural sinusoidal amplitude modulation; NCH nonsimultaneous cross-coincidence histogram; NVIII eighth nerve; PRR pulse repetition rate; SI synchronization index; SON superior olivary nucleus; SPL sound pressure level; TS torus semicircularis.

*Correspondence to:* Ivo H.M. van Stokkum, Faculty of Physics and Astronomy, Free University, De Boelelaan 1081, 1081 HV Amsterdam, The Netherlands.

pulsatile character. The pulses have a duration of 12 ms and a pulse repetition rate which, depending on temperature (Van Gelder et al., 1978), varies between 20 and 40 Hz. The key problems in anuran auditory communication are the identification and localization of calling conspecific males. It has been found that important parameters of the sound for call discrimination are: spectral content (e.g. Capranica, 1966), pulse repetition rate (e.g. Walkowiak and Brzoska, 1982) and pulse shape (Gerhardt and Doherty, 1988). Usually the neural bases for identification and localization of sound are investigated separately. On the one hand selectivity for spectral and fine-temporal characteristics of sound is investigated monaurally on many levels of the auditory system. On the other hand the selectivities for spatial cues like interaural intensity and time differences are investigated with simple stimuli like clicks or pure tones at the neuron's best frequency. In this study we have

combined both approaches. Stimuli with varying amplitude modulation frequency and interaural time difference were presented through a closed sound system. In this way we investigated the combined selectivity for AMF and ITD.

The rationale for the variation of AMF is the periodic pulsatile character of the grassfrog's natural calls. The rationale for variation of ITD however is more indirect. The anuran acoustic periphery acts as a combined pressure-pressure gradient receiver (Aertsen et al., 1986; Feng and Shofner, 1981; Vlaming et al., 1984). Thereby the azimuthal angle of sound incidence is transformed into a frequency dependent interaural intensity difference at the level of both inner ears (Pinder and Palmer, 1983; Vlaming et al., 1984). IIDs which can be as large as 10 dB (Michelsen et al., 1986) are transformed into ITDs in the millisecond range by means of the intensity-latency characteristics of auditory nerve fibres (Feng, 1982). These characteristics vary across NVIII fibres, regardless of their BF (Feng, 1982). Variation of ITD rather than IID allows us to study the effects of differences in response latency between NVIII fibres upon neural responses in the central nervous system independent from the effects of differences in ipsi- and contralateral firing rate.

The complexity of neuronal responses to AM sound bursts increases going from NVIII, via DMN and SON to TS (for review see Walkowiak, 1988). The responses of NVIII fibres are well synchronized to the envelope of the amplitude modulator and their rate characteristics show no selectivity for particular AMFs (Rose and Capranica, 1985). In the DMN the envelope synchronization is retained, but a group of phasic neurons shows a band-pass rate response (Hall and Feng, 1988; Van Stokkum, 1987). This band-pass rate response was related to the fast intensity changes of an envelope modulator of 72 Hz, which resembles the shape of a mating call pulse. In a modelling study (Van Stokkum and Gielen, 1989) it was shown that coincidence detection of converging NVIII fibres with slightly different properties could mimic this preference for fast intensity changes. In the TS, the auditory midbrain, a diversity of rate responses is found (Bibikov and Gorodetskaya, 1981; Rose and Capranica, 1984, 1985). Only one third of the TS neurons shows

significant envelope synchronization (Eggermont, 1990; Epping and Eggermont, 1986b). In a second modelling study (Van Stokkum, 1990) it was made plausible that temporal integration with integration time constants longer than 10 ms (Bibikov 1977, 1978) was responsible for the loss of envelope synchronization. At the same time this temporal integration of model DMN inputs produced a preference for successive fast intensity changes, such as those present in AM tone bursts or natural calls. In this way TS model neurons developed a pronounced band-pass rate characteristic for amplitude modulated tones.

Binaural interaction starts at the level of the DMN (Feng and Capranica, 1976). In DMN and SON (Feng and Capranica, 1978) almost 50% of the cells are binaurally sensitive. In the TS (Feng and Capranica, 1978; Melssen and Epping, 1990) this number is about 80%. In all three nuclei about 10% of the cells receive excitatory input from both ears (EE). The most common type of binaural interaction is contralateral excitation combined with ipsilateral inhibition (EI). The fraction of EI cells increases from 36% (DMN) and 28% (SON) to 60% in the TS. It thus appears that the excitatory input to EI cells in these three nuclei is at least of second order, whereas the inhibitory input is at least of first order. We therefore chose to model an EI neuron receiving excitatory input from DMN neurons and inhibitory input from NVIII fibres. Note that when binaural interaction is incorporated a DMN cell that receives excitatory input from the contralateral DMN and inhibitory input from the ipsilateral NVIII is in fact a third order cell.

The goal of this paper is twofold: to describe the combined selectivity for ITD and AMF found in the TS, and to extend the monaural model for temporally structured stimuli (Van Stokkum, 1989) to a binaural model. A preliminary account has been published elsewhere (Melssen and Van Stokkum, 1988). In this paper special emphasis is put on the difference between monaurally and binaurally determined temporal selectivity. Furthermore a possible influence of neural interaction was investigated by recording simultaneously from single unit pairs.

As an example, the responses of an EI neuron in the TS to a set of monaural and binaural AM

tone bursts will be analysed in depth. Its responses are compared to those of a model EI neuron. It will be shown that the proposed model reproduces the combined ITD-AMF selectivity found with the experimentally observed TS neuron.

## Methods

### *Animal preparation and recording procedure*

Adult grassfrogs (*Rana temporaria* L.) from Ireland were anaesthetized with a 0.05% solution of MS-222. A hole was drilled into the parietal bones above the midbrain, leaving the dura intact. The animal was allowed to recover overnight. The next day it was immobilized with an intralymphatic injection of Buscopan (0.12 mg per gram body-weight). A local anaesthetic, Xylocaine 2%, was applied to the wound margins. The animal was placed in a sound attenuated room (IAC type 1202A) onto a damped vibration-isolated frame. Temperature was maintained around 15°C and the skin was kept moist to aid cutaneous respiration. The animal's condition was monitored by examination of the blood flow in superficial vessels below the dura and with help of ECG recording (Epping and Eggermont, 1987). Thereby constancy of heart rate was interpreted as an indication that no pain was induced. The preparation was usually kept intact for two days.

Ultrafine or tapered tungsten microelectrodes (Micro Probe Inc.), coated with Parylene-c, having a 5–25 µm exposed tip and a 1 kHz impedance of 1–5 MΩ were used for extracellular recording. Using hydraulic microdrives three independent electrodes, tip separation on the roof of the midbrain between 100 and 400 µm, were lowered into the TS and separable few-unit recordings were obtained with help of a spike separation procedure (Epping and Eggermont, 1987). Waveform features and spike epochs were stored on a PDP 11/34 with a resolution of 40 µs, and analysed off-line with a PDP 11/44 and a VAX 11/785.

### *Acoustic stimulus presentation and response analysis*

The acoustic stimuli were generated by a programmable stimulus generator, as described by Epping and Eggermont (1985a). The stimuli were

presented to the animal by two electrodynamic microphones (Sennheiser MD211N) coupled to the tympanic membrane using a closed sound system. In order to decouple both ears, the frog's mouth was kept open during the experiment (Vlaming et al., 1984). The sound pressure level was measured in situ with a half inch condenser microphone (Brüel and Kjær 4143) connected to the coupler. The frequency response of the system was flat within 5 dB for frequencies between 0.1 and 3.2 kHz, which is a sufficient range for studying the auditory system of the grassfrog (Brzoska et al., 1977). The amplitude and phase characteristics of the left and right coupler were equal within 2 dB and 30° (at 0.5 kHz), respectively. Usually, stimuli were presented contralaterally with respect to the recording site, at sound pressure levels of 70 to 100 dB peak. These sound pressure levels are sufficient to evoke behavioural responses (Walkowiak and Brzoska, 1982; Brzoska, 1984). For units with very low thresholds, which could experience internal acoustic crosstalk through the acoustic periphery (Feng and Capranica, 1976), sound pressure levels less than 30 dB above threshold were applied.

The following stimulus ensembles have been used:

### *Amplitude modulated tone bursts with interaural time differences (AMF-ITD)*

The amplitude of a tone burst was sinusoidally modulated with a modulation depth of 100% (Fig. 1a). Carrier phase was set to zero at the beginning of each individual pulse-envelope. AMFs were 9, 18, 36, 72 and 144 Hz. In addition, an unmodulated tone (rise and fall time 5 ms) and a tone modulated by a noise envelope (first row of Fig. 1a) were presented. The AC-component of the noise envelope was obtained by low-pass filtering (48 dB/octave, cut-off frequency at 0.15 kHz) a pseudorandom binary noise sequence (Hewlett-Packard HOI 3722A). The peak modulation depth of the noise envelope was equal to 30 dB (Epping and Eggermont, 1986b). Each tone burst had a duration of 680 ms and was presented binaurally at onset intervals of 3 s. In addition to ipsi- and contralateral presentations, the following ITDs were applied: -5, -3, -1, 0, 1, 3, 5 ms. A negative ITD indicates a leading ipsilaterally pre-

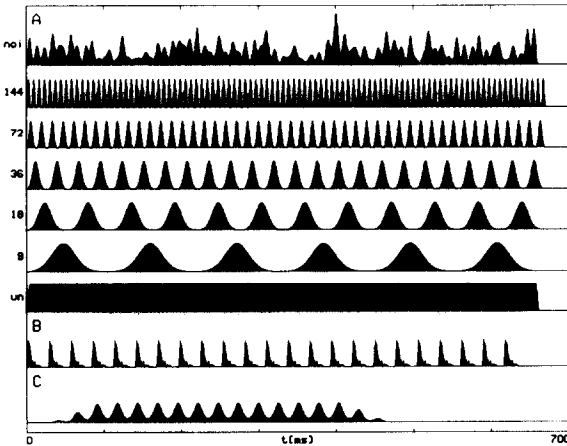


Fig. 1. Stimulus envelopes. (a) Envelopes used with AMF-ITD stimulation. AMF is indicated at the left. The unmodulated (un) and noise envelopes (noi) are depicted as well. (b) Envelope of the artificial mating call used with ITD-call stimulation. (c) Example of a sinusoidally modulated envelope used with MSAM stimulation. Time base, for all stimulus envelopes, is indicated at the lower horizontal axis.

sented tone burst. These 63 different AMF-ITD combinations were presented pseudorandomly. In order to minimize habituation effects, three 36 Hz modulated tone bursts (ITD = 0 ms) were presented first which were excluded from the analysis. In earlier experiments a simpler version of this stimulus was used (Melssen and Van Stokkum, 1988).

#### *Artificial calls with interaural time differences (ITD-calls)*

The artificial call consisted of twenty-three pulses with the natural mating call pulse envelope and with a repetition rate of 36 Hz (Fig. 1b). The following ITDs were applied pseudorandomly: 0,  $\pm 0.3$ ,  $\pm 0.6$ ,  $\pm 0.9$ ,  $\pm 1.2$ ,  $\pm 1.5$ ,  $\pm 2.0$ ,  $\pm 2.5$ ,  $\pm 3.0$ ,  $\pm 6.0$ ,  $\pm 9.0$  ms. To minimize habituation effects, three calls of ITD = 0 ms were presented first which were excluded from the analysis (Melssen et al., 1990).

#### *Monaural sinusoidally amplitude modulated tone bursts (MSAM)*

Tone bursts of 500 ms duration with 100 ms overall rise and fall times were presented every 3 s (Fig. 1c). The modulation depth was 16 dB, corre-

sponding to 84%. The AMFs were varied pseudorandomly between 7.8 and 250 Hz. In addition an unmodulated tone burst was presented (Epping and Eggermont, 1986b).

In general, the stimuli were presented at a unit's best excitatory frequency which was determined with monaurally presented tone pips. To check the reproducibility of the responses and to collect adequate data all stimuli were repeated at least five times. In the figures the responses to the stimuli are presented as reordered event displays and spike rate histograms. Thereby the actual response is reordered systematically according to one or two stimulus parameters. In this paper spike rate is defined as the average number of action potentials per stimulus presentation. In case units were spontaneously active, a time window was applied to separate stimulus evoked events from spontaneous discharges. The time window was estimated from the peri stimulus time histogram. The response latency was defined by the time elapsed between the onset of the pulse train at the excitatory (mostly the contralateral) ear and the first occurrence of a stimulus evoked neural event.

From the ITD-rate histograms, obtained with AMF-ITD and ITD-call stimulation, the so-called cut-off interaural time difference was determined. This CITD, which is defined by the ITD at which the firing rate was reduced to 50% of the maximum in the ITD-rate histogram, serves as a measure of the degree of ITD selectivity.

The degree of time-locking to the stimulus envelope was studied by means of the synchronization index or vector strength (Goldberg and Brown, 1969). The SI was computed from the period histogram belonging to a particular AMF, ITD or AMF-ITD combination. By determining the likelihood value  $2N(SI)^2$ , where  $N$  indicates the number of neural events, the significance of time-locking was tested with the Rayleigh test of circular data (Mardia, 1972). For large values of  $N$  a  $\chi^2$  approximation (degrees of freedom 2, significance level 0.025) was applied.

The presence of neural interaction was investigated by cross-correlation of simultaneously recorded spike trains (Epping and Eggermont, 1987; Melssen and Epping, 1987). Neural synchrony resulted in a peak or trough in the simultaneous

cross-coincidence histogram. The formula for bin  $m$  of the cross-coincidence histogram reads:

$$CCH_{12}(m) = \frac{1}{T\Delta} \int_0^T dt \int_{(m-\frac{1}{2})\Delta}^{(m+\frac{1}{2})\Delta} d\tau z_1(t) z_2(t+\tau) \quad (1)$$

Here  $z_i(t) = \sum_{j=1}^{N_i} \delta(t - t_{i,j})$  represents the events at times  $t_{i,j}$  of neuron  $i$ ,  $T$  is the duration of the experiment and  $\Delta$  is the bin-width of the cross-coincidence histogram. The contribution of a common stimulus influence to this synchrony was estimated by the nonsimultaneous cross-coincidence histogram, also called shift predictor (Perkel et al., 1967). The nonsimultaneous cross-coincidence histogram results from cross-correlation of one unit's spike train with the spike train of the other unit shifted circularly over the length  $L$  of a stimulus sequence (Eq. 2). Hereby it was verified that the responses of the neurons were periodically stationary, i.e. the response probability remained identical for subsequent stimulus sequences.

$$NCH_{12}(m) = CCH_{12}\left(m + \frac{L}{\Delta}\right) \quad (2)$$

A difference between the simultaneous and nonsimultaneous cross-coincidence histogram indicates that the neural synchrony is not merely caused by stimulus influences, but that neural interaction also contributes (Perkel et al., 1967).

### The model

The model for an EI neuron consists of an excitatory contralateral branch and an inhibitory ipsilateral branch. The excitatory branch is equal to the monaural model for TS neurons described in Van Stokkum (1990). The inhibitory branch consists of NVIII fibres which supply inhibitory input to the EI model neuron. The model's components are briefly described below and are shown in Fig. 2. A cascade consisting of a linear middle ear filter (Fig. 2A, impulse response in Eq. 3), a linear band-pass filter (Fig. 2B, impulse response in Eq. 4), and a static nonlinearity (Fig. 2C, Eq. 5) produces a hair-cell potential  $u$ . The middle ear filter, which was derived from Aertsen et al. (1986),

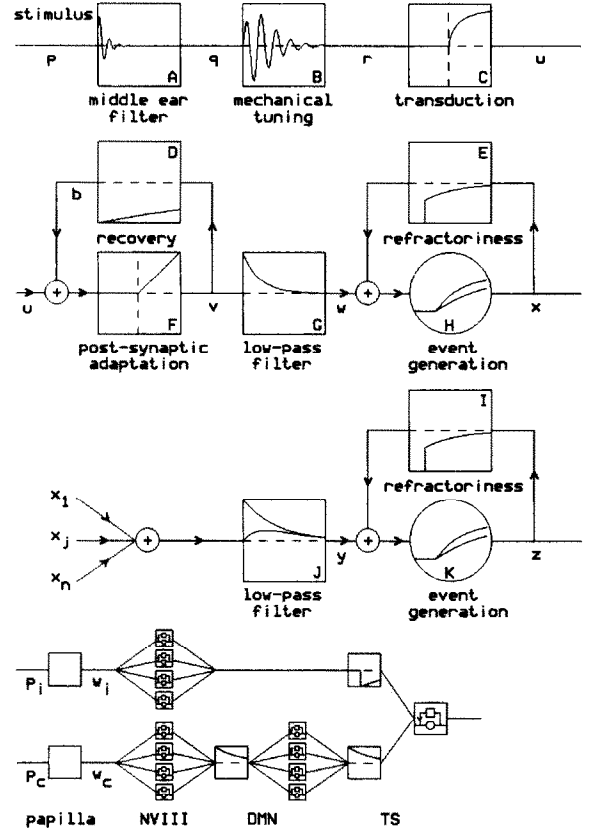


Fig. 2. Model for the processing of sound by the papilla, NVIII, DMN and TS of the grassfrog. The stimulus waveform is band-pass filtered by the middle ear (A), and filtered and transduced into a hair-cell potential (B, C). The synapse between the hair-cell and the dendrite of the NVIII fibre consists of a short-term adaptation mechanism (D, F) and a low-pass filter (G). From the generator potential  $w$  of the NVIII fibre action potentials are generated (H), which form the point process  $x$ . Absolute and relative refractory mechanisms are incorporated in the negative feedback loop (E). Outputs from lower order neurons ( $x_1, \dots, x_j, \dots, x_n$ ) converge upon a higher order neuron, where they add linearly and are convoluted with an EPSP shape (J). From the generator potential  $y$  of the higher order neuron action potentials are generated in the same way as explained above. In Figs. A, B, D, E, G, I and J impulse responses are drawn on a time base of 5 ms. Figs. C and F represent the instantaneous nonlinearities of, respectively, Eqs. 5 and 6. Figs. H, K show probabilities of event generation (Eqs. 9, 11) as function of the generator potentials  $w$ ,  $y$ . The lower flow diagram symbolizes the connections used in the simulations of this paper. The generator potentials  $w_i$  and  $w_c$  are used to generate events in four ipsi- and four contralateral NVIII fibres. Four contralateral DMN units receive NVIII input and provide the excitatory input to the EI neuron, which receives its delayed inhibitory input from the ipsilateral NVIII fibres. One EPSP shape is used in the contralateral branch and another IPSP shape is used in the ipsilateral branch. Further explanation in text.

is described by the resonance frequency  $\omega_1$  and decay rate  $\gamma$ :

$$h(t) = 2\gamma e^{-\gamma t} \sin(\omega_1 t) \Theta(t) \quad (3)$$

with  $\Theta(t) = 1$  if  $t > 0$ , and  $\Theta(t) = 0$  if  $t \leq 0$ . The band-pass filter impulse response  $f_i(t)$  is characterized by a centre frequency  $\omega_i$  and by a time constant  $\beta_i$  which determines the sharpness of the filter.

$$f_i(t) = 2\beta_i^{-2} t e^{-t/\beta_i} \sin(\omega_i t) \Theta(t) \quad (4)$$

Parameter  $r^\circ$  of the mechano-electrical transduction non-linearity (Eq. 5, Fig. 2C) is related to the half-saturation sound pressure level (Crawford and Fettiplace, 1981).

$$u(r) = \frac{r}{r + r^\circ} \Theta(r) \quad (5)$$

The hair-cell potential  $u$  provides the input to an adaptation component which was adopted from Eggermont (1985), and which is described by an inactivation rate  $\lambda$  and a recovery rate  $\mu$  (see Van Stokkum and Gielen, 1989):

$$v = (u + b) \Theta(u + b) \quad (6)$$

$$\frac{db}{dt} = -\lambda v - \mu b \quad (7)$$

The differential equation for  $b$  corresponds to that describing a first-order low-pass filter. Note that omission of the rectifier (Fig. 2F) would leave us with a high-pass filter. Low-pass filtering by the dendrites of the NVIII neuron (Fig. 2G, impulse response in Eq. 8) produces the generator potential  $\omega$  of the first order model neuron.

$$l(t) = \omega_2 e^{-\omega_2 t} \Theta(t) \quad (8)$$

Action potentials (events) are generated stochastically with help of a generator function  $g(w)$ , known in point process literature (e.g. Cox and Isham, 1980) as the intensity function. The probability of event generation in a bin with width  $\Delta t$  is (see Van Stokkum and Gielen, 1989):

$$P[\Delta N(t) = 1] = 1 - e^{-g(w)\Delta t} \quad (9)$$

Here  $N(t)$  is the counting process, which represents the number of events up to time  $t$ , and  $\Delta N(t) = N(t + \Delta t) - N(t)$ . The argument of the generator function depends in two ways on the events generated in the past. Firstly, after an event has been generated the probability per unit of time to generate an event,  $g(w)$ , is zero for an absolute refractory period  $\tau_{abs}$ . Secondly, to model relative refractoriness a negative feedback is supplied to the event generator. This feedback is given by the impulse response  $c(t)$ , which starts after the end of  $\tau_{abs}$ :

$$c(t) = -R e^{-((t - \tau_{abs})/\tau_R)} \Theta(t - \tau_{abs}) \quad (10)$$

Here  $R$  and  $\tau_R$  denote, respectively, the strength and duration of the relative refractoriness. The refractory mechanism is illustrated in Figs. 2E and 2I, with  $\tau_{abs} = 1$  ms and  $\tau_R = 2$  ms. For the generator function  $g(w)$  a semi-linear function is chosen:

$$g(w) = \nu(w - m) \Theta(w - m) \quad (11)$$

When the generator potential  $w$  is less than  $m$ , the threshold parameter,  $g(w)$  is zero. Parameter  $\nu$  determines the slope of  $g(w)$ . In Figs. 2H, K the probability of event generation, which results from substitution of Eq. 11 into Eq. 9, is drawn for two different values of  $\nu$ .

#### Spatiotemporal integration of inputs

The convergence of lower order neurons upon a higher order neuron is modelled as a linear summation of the input point processes. The incoming action potentials are convoluted with the accompanying EPSP or IPSP shape. In formula (Johannesma and Van den Boogaard, 1985):

$$y(t) = \sum_{k=1}^n \int ds e_k(s) x_k(t-s) \quad (12)$$

with

$$e_c(t) = W_c e^{-((t/\tau_{d,c})} (1 - e^{-t/\tau_{w,c}}) \Theta(t) \quad (13)$$

and

$$e_i(t) = W_i e^{-((t-\Delta)/\tau_{d,i})} (1 - e^{-((t-\Delta)/\tau_{w,i})}) \Theta(t - \Delta) \quad (14)$$

Here  $x_k(t) = \sum_{j=1}^{N_k} \delta(t - t_{k,j})$  represents the events at times  $t_{k,j}$  of lower order neuron  $k$ . Note that the ipsilateral contribution  $e_i(t)$  experiences an interaural time delay  $\Delta$  (Eq. 14). In Fig. 2J different EPSP shapes  $e_c(t)$  are drawn. In the lower part of Fig. 2 a schematic diagram for a third order neuron is illustrated. The generator potentials  $w_i$  and  $w_c$  each provide input to four NVIII fibres, which differ in threshold and absolute refractory period. Spatiotemporal integration of the four contralateral NVIII inputs produces a generator potential  $y$  for four DMN neurons which again differ in threshold and absolute refractory period. Finally spatiotemporal integration of these four DMN inputs and the ipsilateral NVIII inputs produces a generator potential  $y$  for the EI neuron. Each model neuron box consists of an event generator and a negative feedback provided by the refractory mechanisms.

#### Implementation of the model

The model was implemented in Fortran 77 on a VAX 11/785 computer. The stimuli were sampled

and provided the input to the model. The sample interval was 0.1 ms for the ITD-call and MSAM stimulus and 0.2 ms for the combined AMF-ITD stimulus. Usually, the number of stimulus presentations differed between real and model neurons.

A summary of the parameters used in the simulations of this paper is given in Table I. To reduce the degrees of freedom the same parameters were used for the ipsi- and contralateral NVIII fibres. The degrees of freedom are: the tuning characteristics, the stimulus amplitude relative to  $r^\circ$ , the degree of spatiotemporal integration (EPSP and IPSP shape) and, most important, the parameters which determine the event generation and refractory properties.

Outputs of the model are the generator potentials  $w$  and  $y$  of, respectively, a first or a higher order neuron, and the time-series  $x$  and  $z$ , which mimic the occurrences of action potentials in, respectively, a first or a higher order neuron. The generator potentials help to understand the action of the several nonlinearities incorporated in the model. The time-series  $z$ , or averages thereof in

TABLE I  
MODEL PARAMETERS

Parameters	Eq.	related to	value
$\gamma, \omega_1$	3	middle ear filter	$1.297 \text{ (ms)}^{-1}, 2\pi \cdot 0.876 \text{ kHz}^a$
$\omega_i, \beta_i$	4	tuning characteristics	$2\pi \cdot 0.625, \text{ kHz } 1 \text{ ms}$
$r^\circ$	5	transduction saturation	1
$\lambda^{-1}, \mu^{-1}$	7	short-term adaptation	12.5 ms, 1000 ms
$\omega_2$	8	dendritic low-pass filter	$1 \text{ (ms)}^{-1}{}^b$
$\tau_{abs}, R, \tau_R$	10	refractory properties	NVIII: 4–7 ms, 2.5, 1 ms DMN: 5–8 ms, 6, 1 ms TS: 6 ms, 6, 1 ms
$m, \nu$	11	event generation	NVIII: 0.0002–0.0008, $500 \text{ (ms)}^{-1}$ DMN: 3.4–4, $2 \text{ (ms)}^{-1}$ TS: 4, 3 $\text{(ms)}^{-1}$
$n$	12	amount of convergence	4
$W_c$	13	EPSP height	2
$W_i$	14	IPSP height	–3
$\tau_{d,c}, \tau_{u,c}$	13	EPSP shape	NVIII → DMN: 4 ms, 0 ms DMN → TS: 4 ms, 0 ms
$\tau_{c,i}, \tau_{u,i}$	14	IPSP shape	NVIII → TS: 5.5 ms, 0 ms
$\Delta$	14	interaural time delay overall time delay	ipsi – contra: 2 ms 19 ms

<sup>a</sup> derived from Aertsen et al. (1986), p. 21, 25; <sup>b</sup> Crawford and Fettiplace (1980), p. 91; Dunia and Narins (1989).

the form of histograms, can directly be compared to experimental data obtained in higher order neurons.

#### Parameter estimation

Both the model flow diagram depicted in Fig. 2 and Table I illustrate the large number of degrees of freedom for the modeller. The characteristics of first and second order model neurons were kept in line with data from the literature and with those used in previous models (Van Stokkum and Gielen, 1989; Van Stokkum, 1990). Special care was taken to produce a similar response pattern. Thereby an overall time delay was used to fit the latency. The EPSP shape was chosen so as to produce an appropriate synchronization capability.

An attempt was made to automate the parameter estimation. Thereby the criterion for the goodness of fit was the relative residual difference  $\epsilon$  of the rate histograms of model and real neuron.

$$\epsilon = \left( \frac{\frac{1}{M} \sum_{j=1}^M (R_m(j) - R_r(j))^2}{\frac{1}{M} \sum_{j=1}^M R_r(j)^2} \right)^{\frac{1}{2}}. \quad (15)$$

Here  $R_r(j)$  and  $R_m(j)$  are the average spike rate of, respectively, the real and the model neuron in response to the stimulus with parameter variation  $j$ .  $M$  is the total number of stimulus parameter variations.

Minimization of  $\epsilon$  (Eq. 15) constitutes a non-linear least squares problem. To solve this we used estimated gradient information. Thereby the dependence of the rate histogram  $R_m$  upon a parameter was estimated by a 5% parameter increase. A new parameter set was chosen according to the Levenberg-Marquardt method (Press et al., 1986). Again care was taken to retain physiologically plausible parameters.

## Results

### *Amplitude modulated tone bursts with interaural time differences*

Experiments were made throughout the year except for the winter season. Single unit record-

ings were obtained from 120 auditory midbrain neurons in 23 grassfrogs, both males and females. Ten units had a maximum response rate which was less than 1/s. These units were not considered for further analyses. Spontaneous activity was exhibited by 34 units (31%), with 80% of these units having spontaneous firing rates smaller than 2/s. The majority (86%) of TS units responded in a stationary way: response properties did not change during stimulation and were reproducible.

First we will illustrate the different response types, which were classified on the basis of the shape of the ITD- and AMF-rate histogram.

Unit 354-400 (Fig. 3a) does not respond to ipsilaterally presented tone bursts. At each ITD, the response rate decreases with increasing AMF and therefore, the selectivity for AMF is termed low-pass. This unit responds weakly to unmodulated tones and tone bursts with the noise envelope. For AMFs in the 9-72 Hz range, the average response rate increases with ITD. Because of the asymmetrically shaped ITD-rate histograms this unit's ITD selectivity was termed  $A_+$ , with the '+' indicating that rate was at maximum in the positive ITD domain. A maximum response rate is found with contralateral stimulation, indicating the presence of inhibitory influences originating from the ipsilateral auditory pathway.

A band-pass selectivity for AMF is visible in Fig. 3b. This spontaneous unit (rate 1.1/s) responded only to AMFs ranging from 18 up to 72 Hz. The maximum of the symmetrically peaked rate histograms was found for ITDs of +1 up to +3 ms. This so-called S type selectivity for ITD (Melssen et al., 1990) is also observable for the noise envelope. Binaural coincidence detection may be involved in this type of response.

Unit 354-080 was sharply tuned to AMFs of 18 and 36 Hz (Fig. 3c). At these AMFs, the ITD-rate histograms are sigmoidally shaped ( $A_+$  type) and corresponding CITDs are +1 and +3 ms, respectively.

Stimulated contralaterally, unit 344-200 responds to each AMF (all-pass). On the one hand, selectivity for ITD is present only with the 36 Hz modulator and with the noise envelope. On the other hand, selectivity for AMF is influenced by ITD: at ITD = -5 ms this unit responds best to low and high AMFs (bimodal type), whereas in

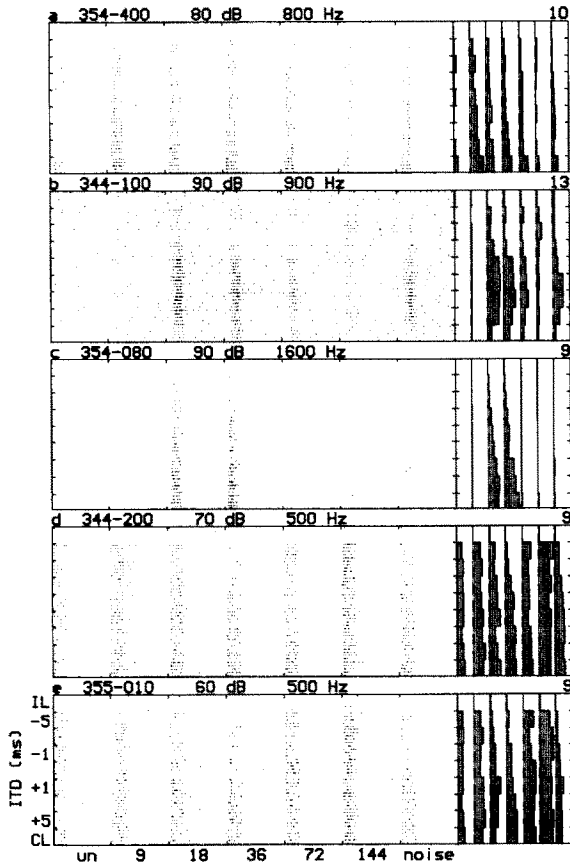


Fig. 3. Responses to combined AMF-ITD stimulation. The event displays were reordered according to AMF (horizontal axis) and ITD (vertical axis). The time between two tick-marks on the horizontal axis is three seconds. The header above each event display indicates unit identification, sound intensity level in dB peak SPL and carrier frequency. For each AMF, average firing rate as function of ITD is represented by the vertical histograms. The scaling number written above the upper-right corner applies to all histograms.

the positive ITD domain no clear selectivity for AMF is observable.

Another example in which selectivity for ITD is influenced by AMF is depicted in Fig. 3e. At 18 Hz a peaked ITD-rate histogram is found (S type) whereas at 36 Hz the ITD selectivity is of the  $A_+$  type. In the rate histogram, corresponding to the 72 Hz AMF, a trough (T type) is visible at ITDs of  $-3$  and  $-1$  ms, respectively. With binaural stimulation, the selectivity for AMF was, for ITDs less than or equal to zero, of the BI type. With positive ITDs there was no clear AMF selectivity.

The distribution of responses is summarized in Table II. The binaural AMF response type was determined from the response to ITD = 0 ms tone bursts. Twelve units which did not respond at this ITD were classified according to their response at a nearby ITD. Examples of these units, which usually were of the BP type, are shown in Fig. 1d,e of Melssen and Van Stokkum (1988).

The most common AMF response types were band-pass (54%) and bimodal (24%). The majority of units responded well to the noise envelope, whereas 15% of the units, which mostly were pronounced band-pass, did not respond to this envelope (e.g. Fig. 3c). One-third of the units (BP or HP) responded weakly or not at all to unmodulated tone bursts.

The ITD response type was judged from the neural responses at an AMF of 36 Hz. Sixteen units not responsive at this AMF were classified at a nearby AMF. Seventy percent of the units had asymmetrical or trough-shaped ITD-rate histograms. These units were excited by one ear and

TABLE II  
DISTRIBUTION OF RESPONSE TYPES WITH AMF-ITD STIMULUS

ITD\AMF	AP	LP	BP	HP	BI	$\Sigma$
NS	2	2	10	2	1	17
$A_+$ , $A_-$ , T	3	5	40	9	20	77
S	0	0	10	1	5	16
$\Sigma$	5	7	60	12	26	110

AMF response types: AP all pass; BP band pass; BI bimodal; HP high pass; LP low pass. ITD response types:  $A_+$ ,  $A_-$  asymmetrical with peak in positive, respectively negative, ITD domain; NS non selective; S symmetrically peaked; T trough.

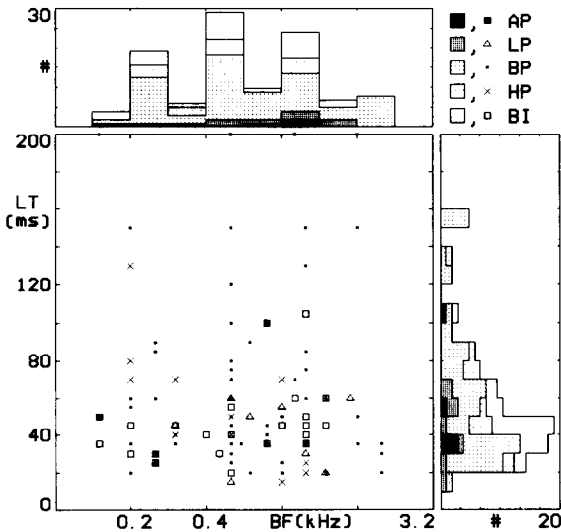


Fig. 4. Distribution of best frequency and latency of the response types found with binaural AMF stimulation. Distributions are represented by a BF-LT scatter diagram and cumulative histograms of BF (horizontal histogram) and LT (vertical histogram). Bin-widths were 0.5 octave and 10 ms, respectively. Meaning of symbols (scatter diagram) and grey-coding (histograms) is indicated at the right of the BF histogram. Four BP units which had latencies larger than 200 ms are not included in the latency histogram. For abbreviations see Table II.

inhibited by the other ear (EI, IE). About 15% of the units had a symmetrically peaked rate histogram, usually with the maximum falling within  $-1$  and  $+1$  ms. This category of units was excited by both ears (EE). The remaining 15% was not selective for ITD.

No relation was present between best frequency and AMF response type (Fig. 4). Except for the band-pass units, no relation between response latency and AMF response type was observed. In the long latency region ( $LT \geq 50$  ms), an overrepresentation of the BP type is evident ( $P < 0.025$ ,  $\chi^2 = 6.5$ ,  $df = 1$ ).

For a detailed account of the relations between BF, LT and ITD response type the reader is referred to Melssen et al. (1990). All units having a symmetrically peaked ITD-rate histogram, possessed BFs well above 0.8 kHz. Units of the other categories had BFs which were uniformly distributed over the applied frequency range. Nonselective units tended to have shorter latencies than

units selective for ITD ( $P < 0.01$ ,  $\chi^2 = 7.41$ ,  $df = 1$ ). For 80% of the units, the selectivity for ITD at an AMF of 36 Hz was comparable to the ITD selectivity observed with noise envelope stimulation. In only a few units, whose responses were restricted to the onset, the response to unmodulated tone bursts was influenced by ITD. An example is visible in the event display of Fig. 10c.

Synchronization to the envelope was classified according to the *SI* as function of AMF. Forty units (36%) exhibited a low-pass synchronization behaviour. A large fraction of these units had cut-off AMFs at 9 Hz ( $N = 21$ ) or 18 Hz ( $N = 9$ ). Ten units (9%) had a band-pass shaped AMF-SI histogram which was at maximum at AMFs of 18 Hz ( $N = 5$ ) or 36 Hz ( $N = 5$ ). Four units exhibited a significant synchronization at all AMFs. The majority of the units (51%), however, showed non-significant SI values at all modulation frequencies.

Thirty-eight units have been tested at two or more intensities over a range of at least 20 dB. Of 4 units (11%) only the selectivity for ITD changed with intensity and of 9 units (23%) only the selectivity for AMF was altered. Of 6 units (16%) the selectivity for AMF as well as for ITD was influenced by sound intensity. The remaining 19 units (50%) had an intensity invariant AMF-ITD selectivity.

A total of 22 units were tested with at least two different carrier frequencies. In general, carrier frequency was varied in steps of 1 octave with respect to BF. Nine units (41%) had comparable selectivities for AMF and ITD at different frequencies. Of 3 units (14%) only AMF selectivity changed with carrier frequency, whereas of 2 units (9%) only the selectivity for ITD was influenced. For the remaining 8 units (36%), the selectivity for AMF as well as for ITD was influenced by carrier frequency.

#### *Comparison between monaural and binaural AMF selectivity*

The small envelope differences between MSAM and AMF-ITD stimulus (compare Fig. 1c and the fourth row of Fig. 1a) did not affect the shape of the monaural AMF rate histogram (nine units tested).

TABLE III  
DISTRIBUTION OF MONAURAL AND BINAURAL AMF  
RESPONSE TYPE

Monaural\Binaural	AP	LP	BP	HP	BI	$\Sigma$
AP	4	1	4	0	5	14
LP	0	3	1	0	2	6
BP	0	1	35	1	1	38
HP	0	0	5	8	2	15
BI	0	2	5	2	14	23
$\Sigma$	4	7	50	11	24	96

In a total of 96 units, the monaural and binaural selectivity for AMF was determined (Table III). Upon monaural stimulation, 16% of the units showed an all-pass response, whereas with binaural stimulation only 4% of the units was nonselective. To compare the distributions of AMF selectivities obtained with monaural and binaural stimulation, we performed a Stuart-Maxwell test (Fleiss, 1988), in which we merged the categories LP, HP and AP of Table III. The two distributions of AMF selectivity differed significantly at the 1% level ( $X^2 = 9.47$ ,  $df = 2$ ).

The monaural and binaural BMFs of BP and BI type units are compared in Fig. 5. The right-hand histogram indicates that most TS neurons had monaural BMFs in the 36–72 Hz range. The scatter diagram shows that, with one exception, monaural and binaural BMFs differed by maximally one octave. For eight BP and four BI units, which had a monaural BMF of 72 Hz, the binaural BMF was one octave lower. Due to this shift, most of the units are tuned to the 36 Hz AMF, which is expressed by the prominent peak in the binaural BMF histogram.

TABLE IV  
INFLUENCE OF PULSE SHAPE AND PULSE REPETITION RATE UPON THE SELECTIVITY FOR ITD

AMF\Calls	NS	A <sub>+</sub> , A <sub>-</sub> , T	S	$\Sigma$
NS	8 (7)	4 (8)	0 (0)	12 (15)
A <sub>+</sub> , A <sub>-</sub> , T	3 (2)	37 (32)	0 (0)	40 (34)
S	0 (1)	4 (4)	3 (3)	7 (8)
NR	1 (2)	1 (2)	0 (0)	2 (4)
$\Sigma$	12	46	3	61

Selectivity for ITD derived from stimulation with artificial mating calls (horizontally) and amplitude modulators of 36 and 72 Hz. The first number applies to the 36 Hz AMF, the second number (between brackets) to 72 Hz.

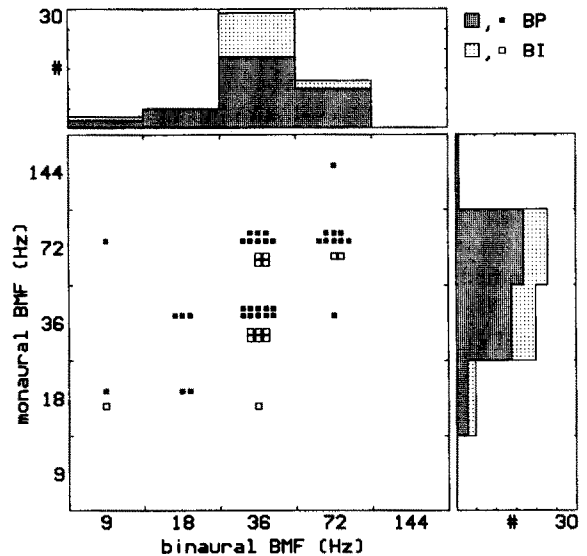


Fig. 5. Distribution of monaural and binaural best modulation frequency for BP and BI type neurons. The monaural BMF was determined with MSAM or AMF-ITD tone bursts presented to the excitatory ear. The binaural BMF was determined from responses to the AMF-ITD tone bursts presented at ITD = 0 ms. The scatter diagram represents the relation between binaural (horizontal axis) and monaural (vertical axis) BMF. Cumulative histograms for binaural BMF (horizontal histogram) and monaural BMF (vertical histogram) are depicted as well (bin-width 1 octave). Meaning of symbols and grey-coding is indicated at the right of the binaural BMF histogram.

#### *Influence of AMF and pulse-shape upon selectivity for ITD*

As has been demonstrated (Figs. 3d,e), the selectivity for ITD may be influenced by the shape of the pulse-envelope and the repetition rate of the individual stimulus pulses. The resemblance be-

tween on the one hand the repetition rate of the pulses in the ITD-call stimulus and the 36 Hz modulator, and on the other hand the rise time of the pulses in the ITD-call stimulus and the 72 Hz modulator (cf. Figs. 1a and 1b), enabled us to examine separately the influences of PRR and rise time upon the selectivity for ITD.

Of 61 units the selectivity for ITD could be determined with the ITD-call stimulus and the 36 and 72 Hz modulators of the AMF-ITD stimulus (Table IV).

The distribution of ITD response types differed significantly between the call and 72 Hz envelope (Stuart-Maxwell test,  $P < 0.025$ ,  $X^2 = 8.33$  df = 2), but not with the 36 Hz envelope ( $P > 0.1$ ,  $X^2 = 4.14$ , df = 2). A few units were not responsive (NR) to AMFs of 36 Hz ( $N = 2$ ) or 72 Hz ( $N = 4$ ).

Of the subset of units which demonstrated the same selectivity for ITD ( $A_+$ ,  $A_-$  or T type) with calls and both AMFs of 36 and 72 Hz, the cut-off ITDs were determined. The differences between, on the one hand, the CITD obtained with ITD-

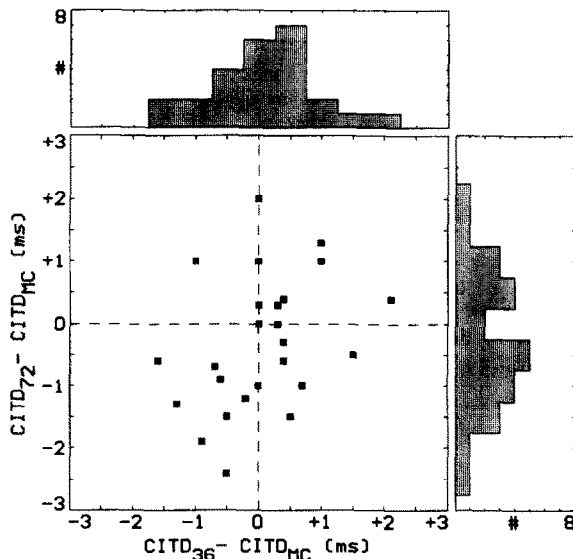


Fig. 6. Distribution of cut-off interaural time differences (CITDs). CITDs were determined from the ITD-rate histograms obtained with ITD-calls ( $CITD_{MC}$ ) and the 36 Hz ( $CITD_{36}$ ) and 72 Hz ( $CITD_{72}$ ) modulators of the AMF-ITD stimulus. The difference in CITD between ITD-calls and the 36 Hz (horizontal axis), 72 Hz (vertical axis) AMFs are represented in the scatter diagram. The bin-width of the cumulative histograms is 0.5 ms. For details the reader is referred to the text.

TABLE V

CROSS-CORRELATION ANALYSIS OF UNIT PAIR RESPONSES OBTAINED WITH COMBINED AMF-ITD STIMULATION

	Recorded on		
	1 electrode	2 electrodes	Total
no synchrony	3	5	8
synchrony	17	35	52
common input	2	6	8

calls and, on the other hand, the CITDs obtained with the 36 and 72 Hz modulators, are represented in Fig. 6. Differences in CITD could be as large as 2.5 ms and were more or less symmetrically distributed as indicated by both histograms. However, with the 36 Hz modulator, 17 out of 25 units (68%) had CITDs which differed by less than 0.5 ms from the CITDs obtained with ITD-calls, whereas with the 72 Hz AMF this number was substantially smaller (44%).

#### Cross-correlation analysis of neural responses

About 55% of the data were obtained while simultaneously recording the activity of two or

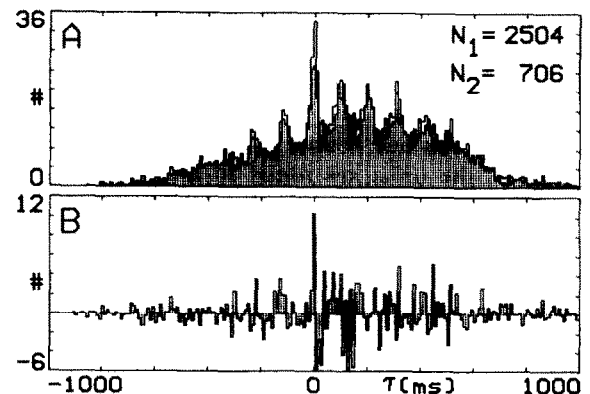


Fig. 7. Cross-correlation analysis of unit pair recordings. The activity of units 342-300 ( $N_1$ ) and 342-020 ( $N_2$ ) was recorded simultaneously during AMF-ITD stimulation on two separate micro-electrodes. (a) Simultaneous and nonsimultaneous (shaded) cross-coincidence histograms. Histograms are normalized for the total number of stimulus sequences. Numbers of events are indicated above the histograms. (b) Difference between CCH and NCH. The time-scale in (b) applies also to (a). Bin-width of the histograms is 10 ms.

more units. Table V summarizes the inferences made from cross-correlations of 60 pairs of units. Most of these units, 52 pairs, showed signs of neural synchrony (Epping and Eggermont, 1987), visible as a peak or trough in the simultaneous cross-coincidence histogram (Fig. 7a). A clear difference between the simultaneous and nonsimultaneous cross-coincidence histogram (Fig. 7b) was seen in 8 of these 52 pairs. The modulation in the *CCH* and *NCH* of Fig. 7a is caused by time-locked responses to some of the AMF-ITD tone bursts. The sharp peak which straddles the origin in Fig. 7b is most probably due to neural common input. The differences between *CCH* and *NCH* in the other seven pairs of units were also ascribed to common input. No clear relation was observed between on the one hand the strength of neural correlation, and on the other hand AMF and ITD. Neither were significant differences observed between unit pair recordings made from one or two micro-electrodes. Thus from cross-correlation analysis no evidence is found for the involvement of neural interaction in the TS (however, see Discussion). In the following a model will be elaborated which predicts responses of a TS unit from convergent input of lower order neurons.

#### Modelling an EI neuron

First it will be shown how the model produces an ITD-selective response to the 36 Hz AM tone bursts by means of spatiotemporal integration of excitatory and inhibitory inputs. Then the complex of selectivities found for a TS unit showing a combined ITD-AMF selectivity will be compared with the model neuron's selectivities. In particular a shift of a monaural BMF of 72 Hz to a binaural BMF of 36 Hz will be demonstrated.

In Figs. 8a and 8b the responses of an ipsilateral NVIII fibre and of a contralateral DMN model neuron (cf. Fig. 2) to the AMF-ITD stimulus are shown. The response in Fig. 8a of the NVIII fibre with the highest threshold and longest  $\tau_{abs}$  shows little selectivity for AMF. The response is smallest for AMFs of 9 and 18 Hz, due to the short-term adaptation. Four NVIII fibres with thresholds varying logarithmically between 0.0002 and 0.0008 and  $\tau_{abs}$  varying linearly between 4 and 7 ms converge upon a DMN neuron. Our

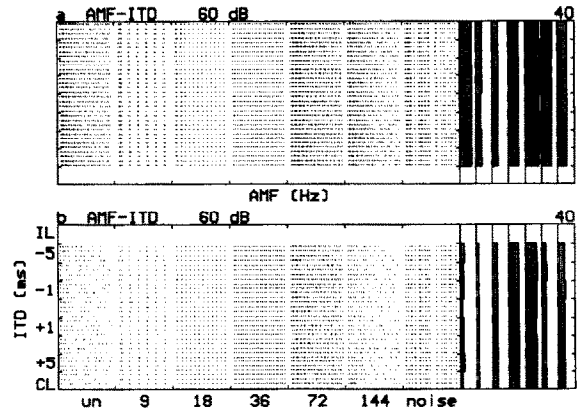


Fig. 8. Response of first and second order model neurons to the AMF-ITD stimulus. Stimulus intensity:  $-18$  dB relative to  $r^\circ$ . Carrier frequency was 0.625 kHz. (a) NVIII fibre with highest threshold ( $m$  0.0008) and longest absolute refractory period ( $\tau_{abs}$  7 ms). (b) DMN neuron which receives input from four NVIII fibres, with  $m$  varying logarithmically between 0.0002 and 0.0008 and  $\tau_{abs}$  varying linearly between 4 and 7 ms. Further DMN model parameters: second order event generation:  $m = 4.0$ ,  $\tau_{abs}$  8 ms. For more details, the reader is referred to the legend of Fig. 3.

model DMN neurons perform a modest degree of coincidence detection (Van Stokkum and Gielen, 1989). The fast intensity changes of the rising phases of the envelope synchronize the NVIII inputs and thus produce a peaked DMN generator potential. In contrast, an unmodulated tone produces a flatter generator potential, because the input firings will gradually become distributed in time, due to their refractory properties. The DMN model neuron in Fig. 8b shows a band-pass rate response with a BMF of 36–72 Hz. The weaker response to the AMF of 144 Hz is due to the different refractory properties of the NVIII fibres. As visible in Fig. 8a the response patterns with the AMF of 144 Hz are nearly as irregular as with the unmodulated tone.

Before we discuss the combined selectivity for AMF and ITD of the model EI neuron, we first illustrate the selectivity for ITD with the 36 Hz amplitude modulator in Fig. 9.

In Fig. 9a the time course of the generator potential  $y$  is depicted as a function of ITD. The upper and lower row show, respectively, the inhibitory and excitatory post synaptic potential. The combination of both with the different ITDs is shown in between. The histograms in Figs. 9b

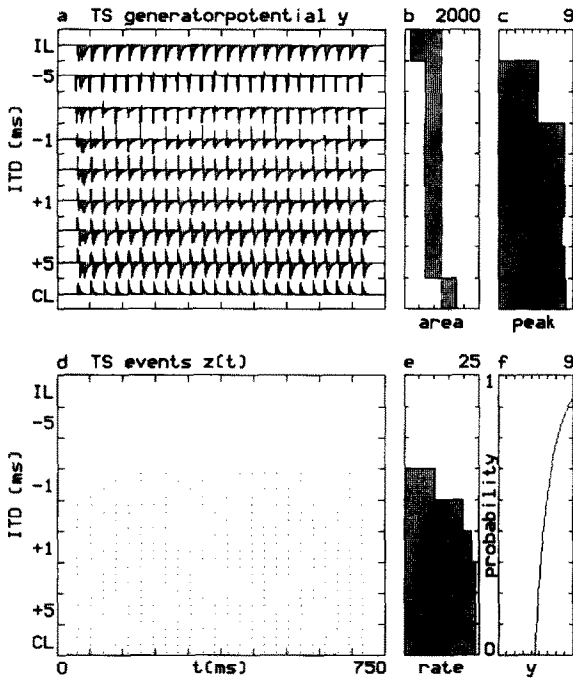


Fig. 9. Simulation of the response of an EI neuron to the binaural variations of the 36 Hz AM tone bursts. The third order model neuron receives inhibitory input from four NVIII fibres as in the 36 Hz column of Fig. 8a and excitatory input from four DMN neurons as in Fig. 8b. The time course of the generator potential  $y(t)$  (a), the area (b) and the peak of  $y(t)$  (c) are depicted as a function of ITD. The probability of event generation (f) is drawn to the scale of (c). Combining the generator potential  $y$  with the event generation and refractory properties results in the reordered event display (d) and rate histogram (e). For model parameters see Table I.

and 9c show, respectively, the area under and peak value of the generator potential as function of ITD. Note that with the stimulus period of 28 ms no temporal summation of EPSPs or IPSPs takes place, because these possess decay times of, respectively, 4 and 5.5 ms. The probability of event generation function (Eqs. 9, 11) in Fig. 9f, which for comparison is drawn to the scale of Fig. 9c, is now used to generate the event display and rate histogram of Figs. 9d,e. In this way a synchronized response results for ITDs larger than 0 ms. In view of the interaural delay  $\Delta$  (Eq. 14) of 2 ms, the suppression of the response with an ITD of  $-1$  ms may come as a surprise. This suppression is caused by the stochastics of the event generation in NVIII fibres and DMN neurons which produces a small jitter. Thus an EPSP which arrives

one carrier frequency period (1.6 ms) later may be overruled by the larger IPSP.

Now we can compare the responses of this EI model neuron with those of a real TS neuron. Unit 343-200 was studied for seven hours. Its selectivities for ITD and AMF are shown in Fig. 10. The unit possessed a best excitatory frequency of 0.6 kHz and a threshold of approximately 40 dB. There were no signs of two-tone inhibition. Response latency was 19 ms. Therefore this unit was modelled with a centre frequency of 0.625 kHz and an overall time delay of 19 ms (Table I). The response to the ITD-calls (Figs. 10a and 11a) shows a clear minimum for ITDs between  $-2$  and  $-6$  ms (T type response). But with an ITD of  $-9$  ms the unit's response is at 70% of the maximum. Thus the effect of the inhibition has nearly worn off after approximately 7 ms (i.e.  $9-2(=\Delta)$ ). To model this, the IPSP decay time  $\tau_{d,i}$  (Eq. 14) was limited to 5.5 ms.

Both rate responses to the MSAM tone bursts (Figs. 10b and 11b) show a weak band-pass char-

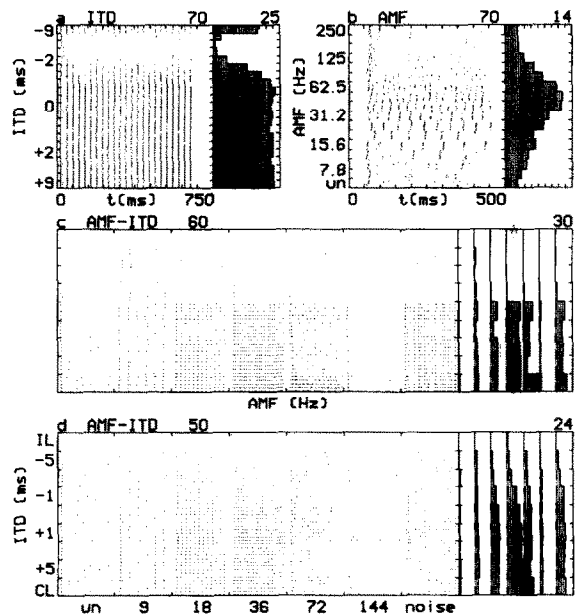


Fig. 10. Responses of TS unit 343-200 to (a) ITD-call stimulus, (b) contralaterally presented MSAM tone bursts and (c, d) AMF-ITD stimulus. The stimulus intensities, in dB peak SPL, are indicated above each event display. Carrier frequency was 0.6 kHz. Time bases are: 750 ms (a), 500 ms (b), and seven times 750 ms (c, d). For more details, the reader is referred to the legend of Fig. 3 and to the text.

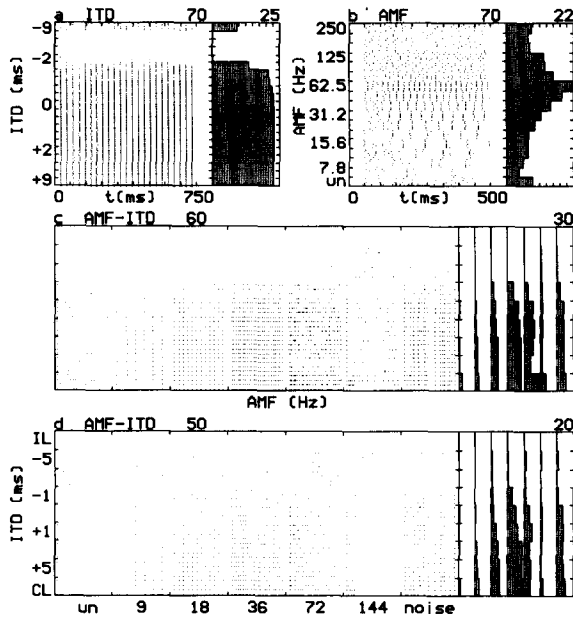


Fig. 11. Responses of the model EI neuron of Fig. 9 to the stimuli of Fig. 10. The response to the 36 Hz AMF in (c) is equal to response depicted in Figs. 9d,e. Carrier frequency was 0.625 kHz. All stimuli were presented at the relative intensities of Fig. 10. The relative residual differences  $\epsilon$  (Eq. 15) between the rate histograms of Figs. 10 and 11 were: (a) 0.14, (b) 0.81, (c) 0.30, (d) 0.41.

acter with a BMF of, respectively, 50 and 62 Hz. However, the model neuron produced nearly twice as many spikes. Now we come to the combined AMF-ITD selectivity which at an intensity of 60 dB is shown in Figs. 10c and 11c. The response to the contralateral AM tone bursts is maximal with an AMF of 72 Hz in both figures. But this BMF shifts to 36 Hz with the binaurally presented stimuli. Focusing on the 72 Hz AMF we observe no response for ITDs less than  $-1$  ms in Fig. 10c nor for ITDs less than  $-3$  ms in Fig. 11c. Furthermore a minimum is visible with an ITD of  $+5$  ms in both figures (fifth column of rate histograms). This is comparable to the circular effect visible in Figs. 10a and 11a. With a stimulus period of 14 ms (72 Hz) an ITD of  $+5$  ms is equivalent to an ITD of  $-9$  ms. In combination with the IPSP decay time of 5.5 ms which produces some temporal summation of the inhibitory inputs the result is a decreased response at an ITD of  $+5$  ms. The main qualitative deviation is found with the 9 Hz AMF where the response of unit

343–200 is only weakly suppressed for negative ITDs. At a 10 dB lower intensity, compare Figs. 10d and 11d, the ITD selectivity becomes less absolute. Some response is visible with ITDs of  $-3$  and  $-5$  ms in Fig. 10d. Note that the monaural response (CL) to the 72 Hz AMF has decreased appreciably in both figures. This effect was already present with the DMN model neurons (not shown).

## Discussion

The aim of the present study was to determine the combined selectivity for amplitude modulation frequency and interaural time difference in auditory midbrain units of the grassfrog. In 82% of the neurons a combined AMF-ITD selectivity was found (Table II). The proposed binaural model reproduced the experimentally observed responses of unit 343–200 to the complete stimulus ensemble successfully. This unit is representative for the largest class, 40 out of 110 neurons, in Table II. In the next sections some implications on the outcome of experiments and simulations will be discussed.

### Selectivity for AMF and ITD

Most units exhibited a band-pass or bimodal response behaviour upon binaural AMF stimulation. A large fraction of these units had a maximal ITD selectivity for AMFs in the range of 36–72 Hz, whereas units seldomly exhibited ITD selectivity in the presence of unmodulated tones. It might be argued that the ITD cue is present only at the onset of the unmodulated tone, and thus one expects only ITD effects with phasically responding units. But then the 144 Hz AM tone, which provides 96 onset ITD cues, is expected to elicit the largest ITD effect. This clearly was not found. It follows from the model study that it is the interplay between the number of onset ITD cues and the intervening interval which determines ITD selectivity. Thereby the pulse shape also exerts an influence (Table IV and Fig. 6).

The distribution of AMF response types obtained with monaural stimulation differed somewhat from the distribution presented in Epping and Eggermont (1986b). In the present study, a

smaller fraction of nonselective units and a larger fraction of high-pass units was found. Presumably, these differences have to be ascribed to the different ways of stimulation: closed mouth (Epping and Eggermont, 1986b) versus open mouth (this study). In the leopard frog Eggermont (1990) studied AMF selectivity with a loudspeaker right behind the frog, which can be compared with our ITD of zero ms. He found more all-pass and less band-pass responders. A reason for this is that we included units which did not respond at an ITD of zero ms. These units usually showed a band-pass response type (Fig. 1d,e in Melssen and Van Stokkum, 1988).

The presence of ITD selectivity in neurons without envelope synchronization was also found in the rabbit midbrain by Batra et al. (1989). Their Fig. 2 can be interpreted as a combined AMF-ITD selectivity.

No clear relations were observed between on the one hand best frequency and on the other hand most of the AMF and ITD response types. Only for units having symmetrically peaked ITD-rate histograms and receiving excitatory input from both ears, BFs were restricted to the high frequency domain. This finding is in agreement with earlier studies on binaural hearing in the grassfrog (Epping and Eggermont, 1985b; Melssen and Epping, 1990; Melssen et al., 1990).

Also no relation was found between latency and AMF and ITD response types, except that units which exhibited a band-pass response behaviour were overrepresented in the long latency domain (see the Discussion below).

#### *Invariance of AMF-ITD selectivity*

In general, TS units exhibit a combined selectivity for frequency and interaural time and intensity difference, which presumably deals with the frequency dependent directionality of the acoustic periphery (Melssen and Epping, 1990; Melssen et al., 1990). Consequently, a consistent determination of sound source laterality can only be achieved by comparing interaural disparities in several frequency bands simultaneously. We found that a considerable number of TS neurons possess such a property: at least 40% of the units exhibits a combined selectivity for AMF and ITD which is not influenced by carrier frequency. Moreover,

about 50% of the units had a combined AMF-ITD selectivity which was invariant with respect to absolute intensity level. The model neuron exhibited a more or less intensity invariant selectivity for AMF and ITD too (Figs. 11c,d).

#### *Mechanisms underlying neural selectivity for AMF and ITD*

In the following we will first discuss the importance of time-locking for the detection of ITDs. Next we deal with the main mechanisms responsible for the combined selectivity for AMF and ITD, namely spatiotemporal integration of excitatory and inhibitory inputs and action potential generation.

#### *Time-locking*

In the DMN strong time-locking to natural and artificial mating call pulses is observed (Schneider-Lowitz, 1983; Van Stokkum, 1987). With binaurally presented artificial mating calls (Melssen et al., 1990) and amplitude modulated tone bursts (e.g. this study), it was revealed that time-locking was exhibited by only a minority of TS units. This is in agreement with earlier studies on temporal selectivity (Eggermont, 1990; Epping and Eggermont, 1986a,b; Rose and Capranica, 1985). The loss of time-locking capability of higher order neurons is due to an increased number of synapses in the pathway between stimulus and recorded neuron (Ribaupierre et al., 1980) and to the presence of temporal integration (e.g. Van Stokkum, 1990). So, considering that time-locking is a prerequisite for an adequate detection of ITD, it is advantageous to process binaural information already in nuclei where a high degree of time-locking is still present. Indeed, in anurans the first binaural interaction takes place at the level of the DMN (Feng and Capranica, 1976).

#### *Modeling ITD selectivity*

In dichotic studies, excitatory and inhibitory influences originating from the ipsi- and contralateral ear upon the neural response pattern have been observed (Carney and Yin, 1989; Goldberg and Brown, 1969; Melssen and Epping, 1990). Binaural modelling studies showed that the selectivity for interaural intensity and time difference is

determined by the time constants of the excitatory and inhibitory neural connectivities (Itoh, 1984; Melssen et al., 1990).

The model flow diagram in Fig. 2 is the simplest way of combining contralateral excitation and ipsilateral inhibition. We found that introduction of DMN elements in the ipsilateral branch did not improve the results, whereas it increased the number of model parameters. Therefore we chose the model of Fig. 2 for EI neurons which show time-locking. Spatiotemporal integration of inputs from such EI neurons can then produce TS neurons which have large integration times (Bibikov, 1977; Van Stokkum, 1990) and show asymmetric forms of ITD selectivity (e.g. Fig. 3c; unpublished model simulations).

Melssen et al. (1990) elaborated upon a model for ITD and IID selectivity, which started from the intensity-rate and intensity-latency characteristics of NVIII fibres measured by Feng (1982). Using spatiotemporal integration of inputs from both ears they could reproduce the different types of ITD and IID selectivity, but only for artificial call stimuli. From their study we infer that the present model can also reproduce the other main type of ITD selectivity, namely the symmetrically peaked response (S) (e.g. Fig. 3b).

#### *Modelling AMF-ITD selectivity*

The majority of TS neurons exhibits a band-pass AMF-rate histogram at an ITD equal or close to zero. About 80% of these units demonstrates also a clear selectivity for interaural time difference. Mostly, due to the combined selectivity for AMF and ITD, the sharpness of AMF tuning in such BP units depends on ITD. Furthermore, these units often had long response latencies. These findings might indicate that spatiotemporal integration of neural activity, originating from ipsi- and contralateral ascending neural pathways, results in an enhanced selectivity for AMF. Indeed, by comparing responses to monaurally and binaurally presented AMFs it was revealed that a considerably lower number of TS units was nonselective for AMF with binaural stimulation. Also a larger fraction of units exhibited a band-pass response behaviour with binaural stimulation.

It was demonstrated in Fig. 11 that the interplay of EPSPs and IPSPs at the model TS neuron

was responsible for the shift in BMF from 72 Hz (monaural) to 36 Hz (binaural). In a previous study (Van Stokkum, 1990) it was shown that temporal integration of successive inputs in combination with a high threshold could produce a pronounced band-pass response (e.g. Fig. 3c). Thus we come to four mechanisms which contribute to AMF selectivity: adaptation in NVIII fibres (Fig. 8a), coincidence detection in DMN neurons (Fig. 8b, Van Stokkum and Gielen, 1989), interference of stimulus periodicity and IPSP decay time (Fig. 11c, 72 Hz AMF), and temporal integration of successive inputs (Van Stokkum, 1990). With all four mechanisms the degree of selectivity is determined by the event generation parameters.

#### *Parameter estimation*

The estimation of model parameters was partly automated, using the relative residual difference criterion of Eq. 15. It appeared that simultaneous estimation of all the involved parameters was unfruitful, therefore we restricted ourselves to the event generation parameters  $\nu$  and  $m$ , and the EPSP decay time  $\tau_{d,e}$ . The  $\epsilon$ -values of Fig. 11, which were obtained with the parameters of Table I, result from a compromise between the responses to the four stimuli. The optimization procedure allowed us to explore the model's possibilities. When for instance only the MSAM stimulus was considered, an increase in the threshold  $m$  from 4 to 5.5, together with decreases of  $\nu$  (from 3 to 2.3  $(\text{ms})^{-1}$ ) and  $\tau_{d,e}$  (from 4 to 2.6 ms) resulted in a decrease of  $\epsilon$  from 0.81 to 0.23.

#### *Neural interaction*

From cross-correlation analysis it was revealed that 87% of the units showed signs of neural synchrony. With monaurally presented temporally structured stimuli, Van Stokkum (1990) arrived at 90%. In this study no evidence was found for the presence of direct excitatory connectivities between TS units, as was observed in 4% of the unit pairs by Epping and Eggermont (1987). But there are two major shortcomings of the cross-correlation method. First, when spontaneous activity is low, as is the case in the TS, inhibition is almost undetectable (e.g. Melssen and Epping, 1987). Second, non-spiking interneurons (e.g. Matsumoto et al., 1986) remain also undetected. Therefore no

hard conclusions can be drawn about the importance of local circuits in the TS for the processing of temporally structured binaural stimuli.

#### *Localization and identification of sound*

In most auditory midbrain units, the selectivities for IID and ITD are intricately coupled (Melssen et al., 1990). Hypothesizing that IID, and thus ITD, corresponds to sound source laterality, the present data provide additional evidence that TS units are involved in the process of sound localization.

The period of the 36 Hz modulator is approximately equal to the interpulse interval of the original mating call of the grassfrog (Van Gelder et al., 1978; Walkowiak and Brzoska, 1982), whereas the rise time of the 72 Hz envelope matches rather well the rise time of mating call pulses. Effects of rise time upon rate selectivity were found in the DMN and, to a lesser extent, in the TS (Hall and Feng, 1988; Van Stokkum, 1987, 1990). A considerable number of TS units with a band-pass or bimodal selectivity for AMF were tuned to the 36 and 72 Hz AMF. This suggests that TS units are also involved in the process of sound identification.

On the one hand at the 36 Hz AMF the strongest influence of ITD upon neural response behaviour was observed. Cut-off ITDs were comparable with 36 Hz AMF and ITD-call stimulation, whereas CITDs could differ substantially with the 72 Hz modulator and the artificial call. On the other hand, comparing responses to monaural and binaural stimulation, a larger number of units was found to be AMF selective in case of binaural stimulation. For units having a band-pass or bimodal selectivity with both kinds of stimulation, a clear shift of BMF towards 36 Hz was observed with binaurally presented AMFs (Fig. 5). Apparently, the 36 Hz periodicity does not interfere with the mechanisms responsible for ITD selectivity, whereas binaural stimulation favours the preference for the 36 Hz AMF. In view of this, we expect that the auditory nervous system is tuned in particular to localize species specific sounds. It is our belief that the use of binaural temporally structured stimuli is a more natural way to investigate the processes of sound localiza-

tion and identification in animals that use stereotyped sounds for intraspecific communication. Summarizing, present data and model simulations indicate that localization and identification of sound are intricately coupled processes which make use of the same underlying neural mechanisms.

#### **Acknowledgements**

This investigation was supported by the Netherlands Organization for Scientific Research (NWO). Koos Braks skilfully prepared the animals. Willem Epping, Stan Gielen, Theis Gootzen, Peter Johannesma and Thom Oostendorp are thanked for helpful discussions or critical reading of the text.

#### **References**

- Aertsen, A.M.H.J., Vlaming, M.S.M.G., Eggermont, J.J. and Johannesma, P.I.M. (1986) Directional hearing in the grassfrog (*Rana temporaria* L.): II. Acoustics and modelling of the auditory periphery. *Hear. Res.* 21, 17–40.
- Batra, R., Kuwada, S. and Stanford, T.R. (1989) Temporal coding of envelopes and their interaural delays in the inferior colliculus of the unanesthetized rabbit. *J. Neurophysiol.* 61, 257–268.
- Bibikov, N.G. (1977) The classification of the neurons in the auditory system on the basis of the function of the expected rate probability. *Akust. Zh.* 23, 346–355.
- Bibikov, N.G. (1978) Dynamics of the expected rate probability in auditory system neurons for different intensities of tonal stimuli. *Akust. Zh.* 24, 816–825.
- Bibikov, N.G. and Gorodetskaya O.N. (1981) Single unit responses in the midbrain auditory center of the frog mesencephalon to amplitude modulated tones. *Neurophysiol.* 12, 185–191.
- Brzoska, J. (1984) The electrodermal response and other behavioural responses of the grass frog to natural and synthetic calls. *Zool. Jb. Physiol.* 88, 179–192.
- Brzoska, J., Walkowiak, W. and Schneider, H. (1977) Acoustic communication in the grass frog (*Rana t. temporaria* L.): calls, auditory thresholds and behavioural responses. *J. Comp. Physiol.* 118, 173–186.
- Capranica, R.R. (1966) Vocal response of the bullfrog to natural and synthetic mating calls. *J. Acoust. Soc. Am.* 40, 1131–1139.
- Carney, L.H. and Yin, T.C.T. (1989) Responses of low-frequency cells in the inferior colliculus to interaural time differences of clicks: excitatory and inhibitory components. *J. Neurophysiol.* 62, 144–161.
- Cox, D.R. and Isham, V. (1980) Point processes. Chapman and Hall, London.

- Crawford, A.C. and Fettiplace, R. (1980) The frequency selectivity of auditory nerve fibres and hair cells in the cochlea of the turtle. *J. Physiol.* 306, 79–125.
- Crawford, A.C. and Fettiplace, R. (1981) Non-linearities in the responses of turtle hair cells. *J. Physiol.* 315, 317–338.
- Dunia, R. and Narins, P.M. (1989) Temporal resolution in frog auditory-nerve fibers. *J. Acoust. Soc. Am.* 85, 1630–1638.
- Eggermont, J.J. (1985) Peripheral auditory adaptation and fatigue: A model oriented review. *Hear. Res.* 18, 57–71.
- Eggermont, J.J. (1990) Temporal modulation transfer functions for single neurons in the auditory midbrain of the leopard frog. *Hear. Res.* 43, 181–198.
- Epping, W.J.M. and Eggermont, J.J. (1985a) Single unit characteristics in the auditory midbrain of the immobilized grassfrog. *Hear. Res.* 18, 223–243.
- Epping, W.J.M. and Eggermont, J.J. (1985b) Relation of binaural interaction and spectrottemporal characteristics in the auditory midbrain of the grassfrog. *Hear. Res.* 19, 15–28.
- Epping, W.J.M. and Eggermont, J.J. (1986a) Sensitivity of neurons in the auditory midbrain of the grassfrog to temporal characteristics of sound. I. Stimulation with acoustic clicks. *Hear. Res.* 24, 37–54.
- Epping, W.J.M. and Eggermont, J.J. (1986b) Sensitivity of neurons in the auditory midbrain of the grassfrog to temporal characteristics of sound. II. Stimulation with amplitude modulated sound. *Hear. Res.* 24, 55–72.
- Epping, W.J.M. and Eggermont, J.J. (1987) Coherent neural activity in the auditory midbrain of the grassfrog. *J. Neurophysiol.* 57, 1464–1483.
- Feng, A.S. (1982) Quantitative analysis of intensity-rate and intensity-latency functions in peripheral auditory nerve fibers of northern leopard frogs (*Rana P. Pipiens*). *Hear. Res.* 6, 241–246.
- Feng, A.S. and Capranica, R.R. (1976) Sound localization in anurans. I. Evidence of binaural interaction in dorsal medullary nucleus of bullfrogs *Rana catesbeiana*. *J. Neurophysiol.* 39, 871–881.
- Feng, A.S. and Capranica, R.R. (1978) Sound localization in anurans. II. Binaural interaction in superior olivary nucleus of the green tree frog *Hyla cinerea*. *J. Neurophysiol.* 41, 43–54.
- Feng, A.S. and Shofner, W.P. (1981) Peripheral basis of sound localization in anurans. Acoustic properties of the frog's ear. *Hear. Res.* 5, 201–216.
- Fleiss, J.L. (1988) Stuart-Maxwell test. In: S. Kotz and N.L. Johnson (Eds.) *Encyclopedia of statistical sciences*, Wiley, New York, Vol. 9, pp. 33–34.
- Gerhardt, H.C. and Doherty, J.A. (1988) Acoustic communication in the green treefrog, *Hyla versicolor*: Evolutionary and neurobiological implications. *J. Comp. Physiol. A* 162, 261–278.
- Goldberg J.M., Brown P.B. (1969) Response of binaural neurons of dog superior olivary complex to dichotic tonal stimuli: Some physiological mechanisms of sound localization. *J. Neurophysiol.* 32, 613–636.
- Hall, J.C. and Feng, A.S. (1988) Influence of envelope rise time on neural responses in the auditory system of anurans. *Hear. Res.* 36, 261–276.
- Itoh, K. (1984) A neuro-synaptic model of bilateral interaction in auditory nervous system. *Trans. IECE Japan* Vol. E 67, No. 1, 12–18.
- Johannesma, P.I.M. and Van den Boogaard, H.P.P. (1985) Stochastic formulation of neural interaction. *Acta Applic. Math.* 4, 201–224.
- Mardia, K.V. (1972) *Statistics of directional data*. Academic Press, London.
- Melssen, W.J. and Epping, W.J.M. (1987) Detection and estimation of neural connectivity based on cross-correlation analysis. *Biol. Cybern.* 57, 403–414.
- Melssen, W.J. and Van Stokkum, I.H.M. (1988) Selectivity for interaural time-difference and amplitude-modulation frequency in the auditory midbrain of the grassfrog. In: H. Duifhuis, J.W. Horst and H.P. Wit (Eds.), *Basic Issues in Hearing*, Academic Press, London, pp. 279–284.
- Melssen, W.J. and Epping, W.J.M. (1990) A combined sensitivity for frequency and interaural intensity difference in neurons in the auditory midbrain of the grassfrog. *Hear. Res.* 44, 35–50.
- Melssen, W.J., Epping, W.J.M. and Van Stokkum, I.H.M. (1990) Sensitivity for interaural time and intensity difference of auditory midbrain neurons in the grassfrog. *Hear. Res.* 47, 235–256.
- Michelsen, A., Jørgensen, M., Christensen-Dalsgaard, J. and Capranica, R.R. (1986) Directional hearing of awake, unrestrained treefrogs. *Naturwissenschaften* 73, 682–683.
- Perkel D.H., Gerstein G.L. and Moore G.P. (1967) Neuronal spike trains and stochastic point processes. II. Simultaneous spike trains. *Biophys. J.* 7, 419–440.
- Pinder, A.C. and Palmer, A.R. (1983) Mechanical properties of the frog ear: Vibration measurements under free and closed-field acoustic conditions. *Proc. R. Soc. Lond. B* 219, 371–396.
- Press, W.H., Flannery, B.P., Teukolsky, S.A. and Vetterling, W.T. (1986) *Numerical recipes*. Cambridge University Press.
- Ribaupierre, F. de, Rouiller, E., Toros, A. and Ribaupierre, Y. de (1980) Transmission delay of phase-locked cells in the medial geniculate body. *Hear. Res.* 3, 65–77.
- Rose, G.J. and Capranica, R.R. (1984) Processing amplitude-modulated sounds by the auditory midbrain of two species of toads: matched temporal filters. *J. Comp. Physiol. A* 154, 211–219.
- Rose, G.J. and Capranica, R.R. (1985) Sensitivity to amplitude modulated sounds in the anuran auditory nervous system. *J. Neurophysiol.* 53, 446–465.
- Schneider-Lowitz, B. (1983) *Neuronaler Verarbeitung einfacher und komplexer Schallsignale in der Peripherie und den unteren Stationen der Hörbahn des Grasfrosches (Rana t. temporaria L.)*. Thesis, Bonn, F.R.G.
- Van Gelder J.J., Evers P.M.G. and Maagnus G.J.M. (1978) Calling and associated behaviour of the common frog, *Rana temporaria*, during breeding activity. *J. Anim. Ecol.* 47, 667–676.
- Van Stokkum, I.H.M. (1987) Sensitivity of neurons in the dorsal medullary nucleus of the grassfrog to spectral and temporal characteristics of sound. *Hear. Res.* 29, 223–235.
- Van Stokkum, I.H.M. (1990) Modelling the response of audi-

- tory midbrain neurons in the grassfrog to temporally structured monaural stimuli. *Hear. Res.* 43, 231–250.
- Van Stokkum, I.H.M. and Gielen, C.C.A.M. (1989) A model for the peripheral auditory system of the grassfrog. *Hear. Res.* 41, 71–85.
- Vlaming, M.S.M.G., Aertsen, A.M.H.J. and Epping, W.J.M. (1984) Directional hearing in the grassfrog (*Rana temporaria* L.): I. Mechanical vibrations of the tympanic membrane. *Hear. Res.* 14, 191–201.
- Walkowiak, W. (1988) Central temporal encoding. In: B. Fritsch et al. (Eds.), *The Evolution of the Amphibian Auditory System*, Wiley, New York, pp. 275–294.
- Walkowiak, W. and Brzoska, J. (1982) Significance of spectral and temporal call parameters in the auditory communication of male grass frogs. *Behav. Ecol. Sociobiol.* 11, 247–252.